FRACTURE MECHANISM OF A BAINITE STEEL IN PRECRACKED AND NOTCHED SPECIMENS AT LOW TEMPERATURE

C. Yan[1], J.H. Chen[2] and Q. H. Qin[1]

[1]Centre for Advanced Materials Technology, School of Aerospace, Mechanical and Mechatronic Engineering, The University of Sydney, NSW2006, Australia
[2]Department of Materials Engineering, Gansu University of Technology, Lanzhou, Gansu, P.R. China

ABSTRACT

Precracked and notched specimens were used to investigate the fracture mechanism of a bainite steel at low temperature. The critical fracture event was studied using metallographic sectioning method. The results showed that the critical cleavage event was different in the precracked and the notched specimens. At -196^{o}C, all specimens fractured at lower-shelf region without any ductile crack growth. The critical crack tip opening displacement was not sensitive to the depth of precrack. With increasing temperature to –100^{o}C, cleavage was preceded by ductile crack growth for all precracked specimens. A longer ductile crack growth was associated with the shallow crack specimens, which resulted in a higher critical crack tip opening displacement. The ratio of depth to width of micro-dimple on ductile crack surface was decreased with ductile crack growth.

KEYWORDS

Fracture toughness, cleavage fracture, crack depth, ductile crack growth, bainite steel, fracture mechanism

INTRODUCTION

Previous research [1-3] showed that metallic materials, especially low-alloy high-strength (HSLA) steels had the different fracture mechanisms at low temperature in precracked and notched specimens. The work of Lin *et al* [2] in AISI 4340 steel showed that with increasing grain size there was an apparent improvement in fracture toughness (K_{IC}) measured using precracked specimens but a decrease in Charpy V-notch impact energy. They attributed this to the variation of cleavage fracture stress and the characteristic distance over which the cleavage fracture can occur. Recently, the work of Chen *et al* on C-Mn steel [4-6] indicated that the cleavage fracture mechanisms were different in a precracked and a notched specimen. Currently, bainite steels have been increasing used in pressure vessels and piping industries due to superior weldability and fracture toughness. However, the fracture mechanisms of bainite steels are still not very clear. In this study, the fracture mechanism of a bainite steel was investigated using precracked and notched specimen at different temperatures. The cleavage fracture toughness and notch

impact energy were measured. The critical cleavage events in precracked and notched were identified using metallographic sectioning methods.

EXPERIMENTAL PROCEDURE

The test material was a bainite steel (WCF-62) in quench-temper condition. The chemical composition is shown in Table 1. The microstructure is tempered bainite. The yielding strength and hardening exponent were measured using round tensile specimen in the temperature range of –196°C to 20°C.

TABLE 1
COMPOSITION OF THE MATERIAL (%)

C	Si	Mn	Ni	Cr	Mo	V	B	S	P
0.06	0.23	1.36	0.36	0.19	0.21	0.03	0.0017	0.009	0.02

Three-point bend specimens with a/W ratio of 0.23, 0.45 and 0.72 were tested at –196°C and –100°C. Crack tip opening displacement (CTOD) at unstable fracture (δ_c) was obtained according to ASTM standard E1290-93. The impact energy was measure using standard Charpy V-notch test from –100°C to 20°C. To investigate the fracture mechanism in both the precracked and notched specimens, the critical fracture event was identified using metallographic method. The critical fracture event is considered as the most difficult step in the process of cleavage fracture from crack initiation to propagation. For the three-point bend specimen, sections were cut perpendicularly to the front of the precrack tip in the specimens unloaded at 95-98% fracture load at which the specimens were regarded in a critical condition. In this study, double-notched four-point bend specimen with the same notch dimensions of Charpy V-notch was used to investigate the critical event in the notched specimen at –196°C. In the double-notched specimens, when cleavage initiates from one notch, the survived notch must be in the critical state due to the same stress condition. The sections are then cut across the survived notch to observe the arrested cleavage microcracks which are shorter than the critical length for unstable propagation. The fracture surfaces were observed using scanning electronic microscope (SEM) and the composition of particles located in cleavage initiation sites was analyzed using energy dispersive analysis of X-ray (EDAX).

RESULTS AND DISCUSSION

Fracture Mechanism of Precracked Specimens at –196°C

The experimental result of the three-point bend (COD) tests at –196°C is summarized in Table 2. P is the failure load, δ_c is the critical crack tip opening displacement, and K_{IC} is stress intensity factor.

TABLE 2
EXPERIMENTAL RESULTS OF COD TESTS AT –196°C

a/W	P (kg)	δ_c (μm)	K_{IC} (kg/mm$^{3/2}$)
0.23	1240	8.32	136.7
0.23	1580	13.9	176.9
0.45	600	7.6	130.2
0.45	620	7.5	129.8
0.45	680	9.8	148.0
0.45	690	9.5	145.7
0.72	280	9.0	142.4
0.72	320	9.2	143.9
0.72	330	8.9	141.7

It can be seen in Table 2 that the fracture toughness is very low and both the δ_c and K_{IC} are not sensitive to the crack depth (a/W). This indicates that all the specimens fractured in the lower-shelf region. The fracture surface is shown in Fig. 1. There are typical river-pattern marks on the fracture surface and the initiation site is very close to the precrack. The EDAX analysis showed that the cleavage initiated from the second-phase particles (1-2μm) rather than non-metallic inclusions. According to the composition of the steel, the second-phase may be carbide or martensite-austenite constituent (M-A). The metallographic analysis by Ikaw *et al* [7] for the similar steel showed that the majority of the second-phase particles were M-A constituents. Fig.2 shows the metallographic section made from the unloaded three-point bend specimen.

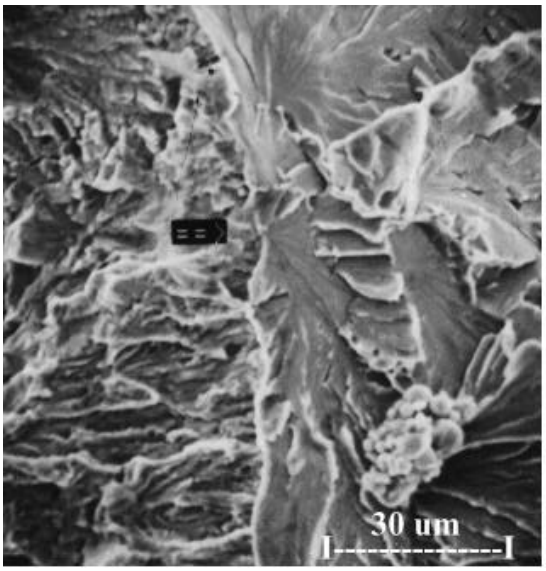

Figure 1: Fracture surface of a three-point bend specimen at –196°C.

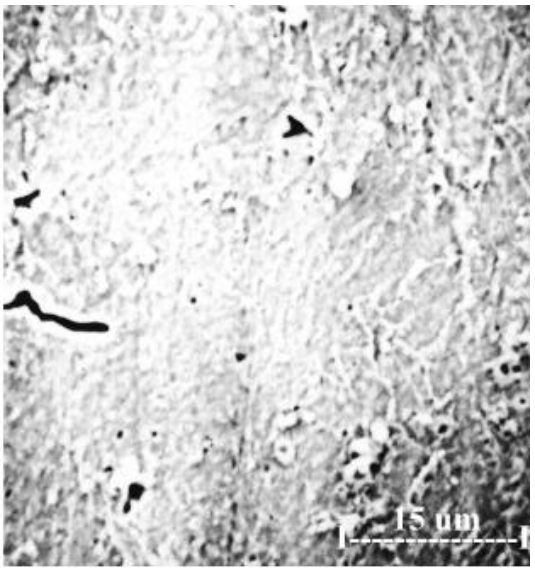

Figure 2: Remaining micro-cracks in the vicinity of precrack tip.

It can be observed in Fig. 2 that the crack tip is only slightly blunted. In the vicinity of the crack tip, some remaining micro-cracks with 1-2μm in length were observed due to unloading prior to fracture. This indicates that the critical fracture event is the propagation of second-phase sized crack to the matrix.

Fracture Mechanism of Precracked Specimen at –100°C

The experimental result of the three-point bend tests at –100°C is shown in Table 3, where δ_u is the crack tip opening displacement at the failure load.

TABLE 3
EXPERIMENTAL RESULTS OF COD TESTS AT –100°C

a/W	P (kg)	δ_u (mm)
0.23	2860	0.635
0.23	2890	0.288
0.23	3280	1.159
0.45	1464	0.413
0.45	1480	0.341
0.72	470	0.096
0.72	510	0.250

In contrast to the fracture at -196°C, for all specimens cleavage was preceded by ductile crack growth. In other words, there was a transition from ductile crack growth to cleavage fracture. It can be seen in the

Table 3 that the average value of δ_u is much higher than the average δ_c (Table 2) due to the ductile crack growth. Also, the δ_u is sensitive to the depth of precrack (*a*/*W*). A high δ_u is associated with a specimen with shallow precrack. Fig. 3 shows the effect of the depth of precrack on the ductile crack growth length (DC). The total length of crack, i.e., precrack plus ductile crack growth (DC+*a*) corresponding to the failure load is also included.

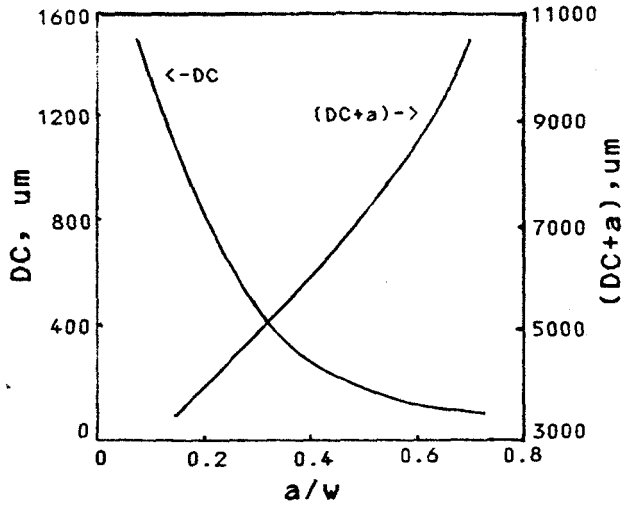

Figure 3: Effect of *a*/*W* on ductile crack growth

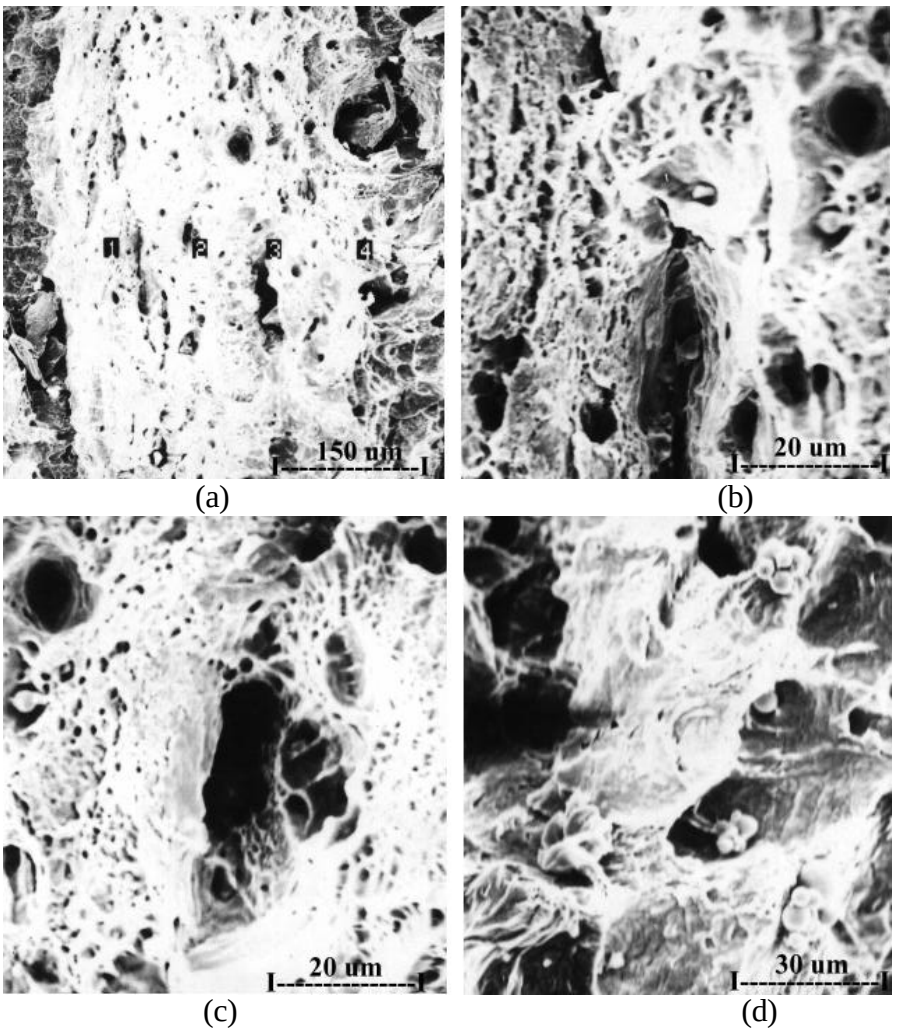

Figure 4: Shapes of microdimples located at different positions of a ductile crack: (a) general view, (b) position 1, (c) position 2 and (d) position 3.

The shallow crack specimen has a greater length of ductile crack growth compared to the deep crack specimen. Normally, fracture toughness is proportional to the length of ductile crack in which the plastic deformation energy is dissipated [8]. The shallow crack specimen has a greater ductile crack growth, thereby having a higher fracture toughness (δ_u). It is well recognized that cleavage fracture is controlled by critical opening stress [9]. Many numerical investigations have demonstrated that the crack depth (a/W) has a significant effect on the stress triaxiality ahead of crack tip [10-11]. The hydrostatic stresses are larger for deeper cracks. On the other hand, Yan *et al* [12] showed that ductile crack growth could elevate the stress triaxiality and opening stress on the remaining ligament. Therefore, a larger ductile crack growth is expected for the shallow crack specimen to raise the opening stress to the critical cleavage stress. The work of Chen *et al* [13] showed that the variation of stress triaxiality could affect the shape of micro-dimples (the ration of depth to width) on the ductile crack surface. High stress triaxiality results a small ratio of depth to width. Fig. 4 shows the variation of microdimples located in different growth length of the ductile crack. In Fig. 4, the dimple becomes flat with the ductile crack growth. This means that the ratio of depth to width of the dimples decreases with ductile crack growth due to an increase of stress triaxiality.

Fracture Mechanism in Notched Specimen

The double-notched four-point bend specimens were tested at –196°C. The fracture surface was typical cleavage fracture without any ductile crack growth. The metallographic sections made from the double-notch four-point bend specimens are shown in Fig. 5. The remaining micro-cracks are much longer than that in the unloaded three-point bend specimens. The typical length of the remaining cracks is about the width of bainite bundle. This implies that the critical cleavage event in the notch specimen is the propagation of grain-sized crack to the matrix, which is, obviously, different from the critical event in the precracked specimen. Cleavage fracture stress can be related to the critical crack size in terms of the well-known Griffith's equation,

$$\sigma_f = \left[\frac{4Er_p}{\pi(1-\nu^2)C}\right]^{1/2}, \qquad (1)$$

where σ_f, E, r_p, ν and C are cleavage stress, Young's modulus, surface energy, Possion's ratio and the critical crack size, respectively. Clearly, a higher cleavage stress can be obtained by decreasing the critical crack size C. As the critical event is the propagation of bainite bundle-sized crack to the matrix, a higher fracture toughness is expected when the size of bainite bundle is reduced.

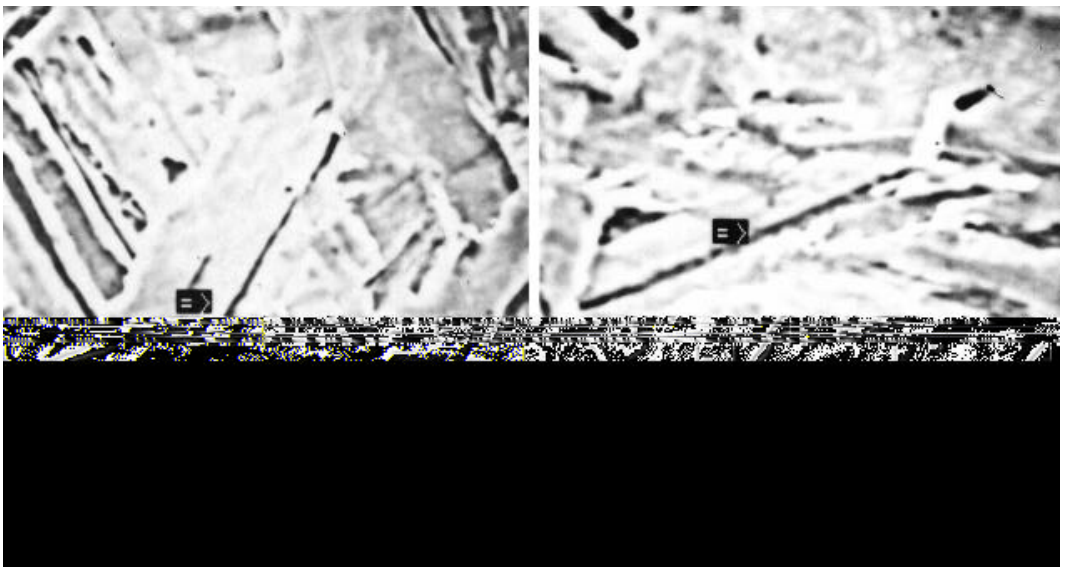

Figure 5: Remaining micro-cracks in the vicinity of notch tip

The impact energy measured in Charpy V-notched specimen from –100°C to 20°C is shown in Table 4.

TABLE 4
CHARPY IMPACT ENERGY (*J*) FROM –100°C TO 20°C

T°C	-100	-80	-60	-40	-20	0	20
	30.8	40.2	40.5	133.9	191.4	184.8	228.0
Impact	32.0	50.6	91.2	1433.0	159.7	187.8	232.1
energy	30.1	49.1	74.9	150.3	181.4	231.6	229.3
	13.1	39.5	86.7	116.2	151.8	203.1	234.0
Average	26.5	44.9	73.3	135.9	171.1	201.8	230.9

It can be seen that there is an increase of impact energy with temperature. The lower-shelf temperature is about –100°C.

CONCLUSIONS

The fracture behaviour of a bainite steel at low temperature was investigated using precracked and notched specimens. Experimental results showed that the critical cleavage events were the propagation of second phase-sized and bainite bundle-sized micro-cracks to the matrix for the precracked and the notched specimens, respectively. At -196°C, both the precracked and the notched specimens fractured at lower-shelf region without any ductile crack growth. The critical crack tip opening displacement was not sensitive to the depth of precrack. At –100°C, for all precracked specimens cleavage was preceded by ductile crack growth. A longer ductile crack growth was associated with the shallow crack specimens, which resulted in a higher critical crack tip opening displacement. The ratio of depth to width of micro-dimple on ductile crack surface was decreased with ductile crack growth, which indicated an increase of stress triaxiality ahead of a growing crack.

REFERENCES

1. Ritchie, R.O. and Horn, R. M. (1978) *Metall. Trans*. 9A, 331.
2. Lin,T., Evans, A.G. and Ritchie, R.O. (1987) *Metall. Trans*. 10A, 641.
3. Zeman, J., Role, S., Buchar, J. and Pokluda, J. (1990) In: *Fracture Mechanics, ASTM STP 1074*, pp396-418, ASTM, Philadelphia.
4. Chen, J.H. and Yan, C. (1992) *Metall. Trans*. 23A, 2549.
5. Yan, C., Chen, J.H., Sun, J. and Wang, Z. (1993) *Metall. Trans*. 24A, 1381.
6. Chen, J.H., Wang, G.Z., Yan, C., Ma, H. and Zhu, L. (1997) *Int. J. Fract*. 83, 105.
7. Ikaw, H *et al* (1980) *Trans. JWS*. 11, 3.
8. Thomason, P.F (1990). *Ductile Fracture of Metals*, Pergamon Press, Oxford.
9. Ritchie, R.O., Knott, J.F. and Rice, J.R. (1973) *J. Mech. Phys. Solids*. 21, 395.
10. Sorem, W.A., Dodds, R.H. and Rolfe, S.T. (1991) *Int. J. Fract*. 47, 105.
11. Ruggieri, C. and Dodds, R.D. (1996) *Int. J. Fract*. 79, 309.
12. Yan, C., Mai, Y.W. and Wu, S.X. (1997) *Int. J. Fract*. 87, 345.
13. Chen, J.H., Wang, G.Z., Yan, C., Ma, H. and Zhu, L. (1997) *Int. J. Fract*. 83, 121.